

Accurate and Facile Determination of the Index of Refraction of Organic Thin Films Near the Carbon 1s Absorption Edge

Hongping Yan,¹ Cheng Wang,² Allison R. McCarn,^{1,*} and Harald Ade¹

¹Department of Physics, North Carolina State University, Raleigh, North Carolina 27695, USA

²Advanced Light Source, Lawrence Berkeley National Lab, Berkeley, California 94720, USA

(Received 3 September 2012; revised manuscript received 22 February 2013; published 23 April 2013)

A practical and accurate method to obtain the index of refraction, especially the decrement δ , across the carbon 1s absorption edge is demonstrated. The combination of absorption spectra scaled to the Henke atomic scattering factor database, the use of the doubly subtractive Kramers-Kronig relations, and high precision specular reflectivity measurements from thin films allow the notoriously difficult-to-measure δ to be determined with high accuracy. No independent knowledge of the film thickness or density is required. High confidence interpolation between relatively sparse measurements of δ across an absorption edge is achieved. Accurate optical constants determined by this method are expected to greatly improve the simulation and interpretation of resonant soft x-ray scattering and reflectivity data. The method is demonstrated using poly(methyl methacrylate) and should be extendable to all organic materials.

DOI: [10.1103/PhysRevLett.110.177401](https://doi.org/10.1103/PhysRevLett.110.177401)

PACS numbers: 78.20.Ci

The complex index of refraction describes the fundamental interaction, i.e., absorption and dispersion, of electromagnetic radiations with materials. These interactions in turn afford and support a plethora of materials characterization tools. Quite often, the quality of the analysis and optimization of experimental procedures or the exploitation of materials in applications ranging from devices to optical elements greatly benefit from an accurate knowledge of the complex index of refraction of the materials investigated. For this reason, optical constants of atoms and materials are catalogued and tabulated over the full range of the electromagnetic spectrum. In the energy range of 50–30 000 eV, the optical constants have been compiled by Henke *et al.* in the form of atomic scattering factors $f(\omega) = f_1(\omega) - if_2(\omega)$ [1], which can be related to the scalar complex index of refraction $n(E) = 1 - \delta(E) + i\beta(E)$ for disordered materials. A well-known limitation of the Henke data is the lack of fine spectral details to describe the optical properties near absorption edges. This is true for atoms, but even more so for compounds, for which the molecular bonding has to be taken into account. For organics, the materials of primary concern here, the near edge x-ray absorption fine structure (NEXAFS) has been compiled for numerous substances by a number of researchers as a supplement to the Henke database [2–8]. Despite the remarkable richness of spectral features in these materials shown in the NEXAFS spectra, the corresponding databases and compilations for the dispersion properties are entirely lacking, other than a few reports on characterizing the dispersion of polyimide and amorphous carbon [9–11].

The recent development and utilization of resonant soft x-ray reflectivity (R-SoXR) and resonant soft x-ray scattering (R-SoXS) [12–18] has posed a greater need for precise knowledge about optical constants of related materials such

as polymers. The strength of R-SoXR and R-SoXS is based on the strong elemental and chemical specific oscillations of the complex index of refraction of polymers near the absorption edge. Within the resonant region, both the relative dispersive and absorptive properties of matter are important and can be selectively employed by simply tuning to the corresponding photon energies. Accurate knowledge of the complex index of refraction is a key aspect of utilizing R-SoXR and R-SoXS productively. Detailed knowledge of δ for a large range of materials will not only benefit R-SoXR and R-SoXS applications, but should be of wider interest, including for phase sensitive x-ray imaging methods [19].

In this Letter, a facile yet accurate method to determine the index of refraction of a polymer material near the carbon 1s absorption edge is presented. This method takes advantage of the fact that the NEXAFS of polymers can be relatively easily measured and, most importantly, that optical properties, i.e., δ and β , are directly fitted in model refinements of thin film reflectivity data. This allows the use of the doubly subtractive Kramers-Kronig (DSKK) method to calculate δ from β accurately.

The absorption part of the index of refraction β can be easily measured in transmission geometry by applying Beer's law $I = I_0 \exp(-4\pi\beta z/\lambda)$, where I_0 is the incident intensity, I is the transmitted intensity through the film of thickness z , and λ is the wavelength in vacuum. If z is accurately known, β can be obtained directly. The relative absorption can also be measured indirectly by using total electron yield measurements, although such a measurement is only semiquantitative [5,20–24]. In contrast, the dispersion part of the index of refraction δ is significantly more difficult to measure with high accuracy, especially for the fine structures near an absorption edge. Interferometry, ellipsometry, and reflectivity have been previously utilized

to determine δ , and to a lesser extent β , for a limited number of materials [9,10,25–28]. For soft x rays, the direct measurement of δ is complicated by the short wavelength (comparing to visible light), the small value of δ , and the relatively strong absorption. Although several types of interferometers have been developed to measure δ by measuring the phase shift of transmitted light through a thin film of the material of interest [9,10,25,29], it is difficult to make interferometric measurements at, or close to, an absorption edge due to the high attenuation of soft x rays [29]. These measurements also require an independent determination of the mass thickness of the film. An alternative way of measuring δ is by fitting the reflectance profile of a solid's surface to the Fresnel reflectivity to extract values for both δ and β . However, sample roughness and high absorption are known to affect the accuracy of these results [24]. Besides, the accuracy is also decreased for larger ratios of β over δ .

The real and imaginary parts of the index of refraction are related through the Kramers-Kronig (KK) relations within a semiclassical description of photon-material interaction [30] (see the Supplemental Material [31] for mathematical details). To avoid the relatively large error brought about by the substitution of the infinite integration energy range with a practically feasible finite range, we employ the subtractive method first introduced by Bachrach and Brown [32]. Specifically, we use the doubly subtractive Kramers-Kronig method to calculate δ from β [33]:

$$\begin{aligned} & \frac{\delta(E)}{(E^2 - E_a^2)(E^2 - E_b^2)} - \frac{\delta(E_a)}{(E^2 - E_a^2)(E_a^2 - E_b^2)} \\ & - \frac{\delta(E_b)}{(E_b^2 - E^2)(E_a^2 - E_b^2)} \\ & = -\frac{2}{\pi} P_C \int_{E_{\text{Min}}}^{E_{\text{Max}}} \frac{E' \beta(E')}{(E'^2 - E^2)(E'^2 - E_a^2)(E'^2 - E_b^2)} dE'. \quad (1) \end{aligned}$$

In this equation, the infinite integration interval is substituted by the finite range from E_{Min} to E_{Max} . The required two known δ values at E_a and E_b can be measured from reflectivity experiments as discussed below.

To further reduce the error caused by the limited energy range, the NEXAFS absorption spectrum is expanded using a “molecular scattering factor” constructed from the Henke atomic scattering factors to span the 10 to 30 000 eV range of the integration variable. Although the readers are referred to the Supplemental Material [31] for detailed procedures, the overall method is described as follows: 1. $\beta_S(E)$ is calculated from the NEXAFS spectrum that is extended with the Henke database. Here $\beta_S(E)$ is defined as $\beta(\rho, E)/(\rho/\rho_0)$, with $\rho_0 \equiv 1 \text{ g/cm}^{-3}$ with the density ρ a scale factor that needs to be determined to obtain β . 2. Using the DSKK method with two required values $\delta(E_a)$ and $\delta(E_b)$ obtained from reflectivity experiments at below-edge and above-edge energies, respectively, this preliminary β is utilized to predict the energy

dependence of δ , which will then need to be scaled with the same scaling factor ρ . 3. ρ is obtained by comparing the reflectivity-measured δ at more energies (far away from the absorption edge) to the predicted δ from last step. 4. ρ is then used to correct both β and the predicted δ for energies in between E_a and E_b . In this procedure, values of δ , instead of β , are used to determine the density. This is because δ is strongly energy dependent even when β is close to zero at below-edge energies (very little absorption), which allows an accurate determination of the density in step 3 by comparing the reflectivity-measured to the DSKK-predicted δ at both below-edge and above-edge energies, where the reflectivity measurements of δ and β are more precise.

The material utilized to demonstrate the methodology is the ubiquitous polymer poly(methyl methacrylate) (PMMA), which is an amorphous polymer that does not show any anisotropy in the index of refraction and can be readily processed into a thin film. The NEXAFS spectra of PMMA were acquired at beam line 5.3.2.2 at the Advanced Light Source (ALS) [34]. PMMA was spun cast from *n*-butyl acetate with a thickness of ~ 70 nm. The film was then floated off in deionized water and picked up with a TEM grid for NEXAFS spectra data acquisition. The absorption spectrum was measured from 270 to 400 eV in transmission. The samples for the reflectivity measurements were prepared from the same solution but on freshly cleaned silicon substrates. Reflectivity (θ - 2θ geometry) data were acquired at the ALS beam line 6.3.2 in a high vacuum [35], following previously established protocols [12] that include precautions to avoid radiation damage which causes spectral changes [36]. Simulations and fits of reflectance were performed using the noncommercial program IMD [37] using a least-squares algorithm.

A molecular scattering factor $f_{2,\text{C}_5\text{H}_8\text{O}_2}$ for PMMA (chemical formula $\text{C}_5\text{H}_8\text{O}_2$) is the sum of the Henke atomic scattering factors of 5 C, 8 H, and 2 O atoms. The calculated β_S from the experimental NEXAFS spectrum and from $f_{2,\text{C}_5\text{H}_8\text{O}_2}$ are plotted in Fig. 1. The NEXAFS data cover an energy range of 270–400 eV, while $f_{2,\text{C}_5\text{H}_8\text{O}_2}$ ranges from 10 to 30 000 eV. The step at ~ 285 eV, also referred to as the absorption edge, is due to the excitation of the core electron into the vacuum continuum. Since no molecular structure is considered in the Henke data, the edge looks like a step function with no details near the edge. The β_S calculated from $f_{2,\text{C}_5\text{H}_8\text{O}_2}$ was then used to expand the NEXAFS spectra for energies lower than 270 eV and higher than 400 eV (see the inset of Fig. 1). The real part of the index of refraction δ then needs to be calculated using the KK relations. To determine the density ρ mentioned above, R-SoXR was performed on a ~ 70 nm PMMA film on a silicon substrate. Reflectance measurements with θ from 0° to 20° were performed for a set of energies spanning the 270–310 eV range (see Fig. 2). Due to the strong energy dependence of the index of refraction,

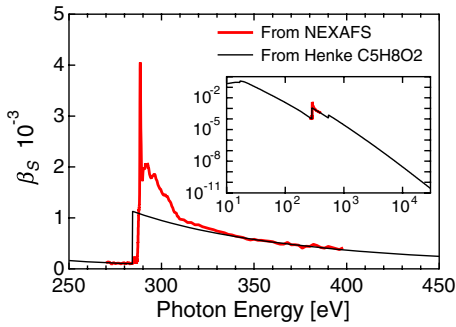


FIG. 1 (color online). Absorption spectra β (assumed density of 1 g/cm^3) calculated from transmission NEXAFS measurements and the Henke atomic scattering factors. The inset shows the same plot with a broader energy range.

the resultant resonant aspects can be readily observed in the reflectance profiles. Below 285 eV, the reflectance profiles have strong Kiessig fringes at all angles. The onset of the first dip in the reflectance profile relates to the critical angle θ_c of the vacuum-PMMA interface, with $\theta_c \approx \sqrt{2\delta}$. For energies above the absorption edge, the reflectance profiles appear less modulated, especially at low grazing angles. This is due to the high absorption of the polymer at these energies and the long optical path the x rays need to travel at small grazing angles. The reflected intensity corresponding to the polymer-substrate interface is reduced, leading to the small Kiessig fringe amplitudes at small angles. At higher angles, the optical path is shorter and less light is absorbed, which leads to better visibility of the interference fringes.

The experimental reflectance profiles are fitted through model refinements of a single layer by means of a least-squares algorithm. It is most advantageous to start by fitting the reflectance data acquired at photon energies far below the absorption edge, e.g., 270 eV, where the sensitivity to δ

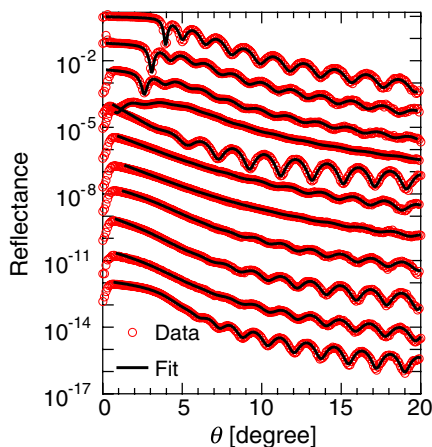


FIG. 2 (color online). Overplot of R-SoXR data (circle) and fits (line) for PMMA single layer, showing the quality of fits at energies of, from top to bottom, 270, 282, 284, 286, 287.6, 288, 288.2, 288.6, 289, 294, and 310 eV.

is high. Parameters that describe the property of the film, such as the film thickness, roughness of the surface, and roughness at the polymer-substrate interface can be extracted with high accuracy. Since all data were obtained from the same sample, these structural parameters can then be used for fitting the reflectance profiles at all other energies. Therefore, only two variables, δ and β , are left as free parameters to be determined by a least-squares fit.

With the values of δ obtained, the density of the PMMA thin film is determined by comparing the values derived from the reflectivity measurement to the DSKK predicted (see the Supplemental Material [31]). From this linear fit, the density of the film is determined to be $1.20 \pm 0.02 \text{ g/cm}^3$ {according to Eq. (10) in the Supplemental Material [31]}, which is very close to the tabulated value 1.18 g/cm^3 and falls into the literature values ranging from 1.17 to 1.22 g/cm^3 . The value of the density is then subsequently used to calculate the accurate β with $\beta = (\rho/\rho_0)\beta_s$, followed by the application of the DSKK method for the calculation of δ . β and δ are plotted in Fig. 3, along with the experimental results from fits of the reflectance measurements at key energies. The error bars in the experimental δ and β reflect the data scatter from fitting results obtained at multiple sample locations, which capture both the error of the fits themselves and the variations that come from the sample. Below the absorption edge, in the energy range of 270–287.6 eV, the values of δ and β from the experiment and from the Kramers-Kronig calculations match well, and the experimental scatter for δ is small. For energies between 290 and 310 eV, systematic errors are observed. The present reflectivity fits slightly overestimate β and underestimate δ . This systematic error can be clearly seen by comparing the fits and data at the onset of the visibility of the Kiessig fringes in Fig. 2. The data show the onset of fringes at smaller angles than the fit, indicating that the model fits overestimate the absorption in the actual films. For comparison, δ and β as derived from the Henke database are also shown in Fig. 3. We note that our method measures the film as prepared, which might contain impurities from the supplier or a small amount of solvent despite the vacuum drying at elevated temperature [38,39]. As the same film has been investigated by reflectivity and by transmission NEXAFS measurements, it is really the agreement between these measurements (related via the KK transform) that is important. Careful inspection actually shows a small peak at around 285 eV that should not be there for pure PMMA. This peak is usually due to C=C π^* resonance according to Stöhr [20]. Considering the solvent used here (*n*-butyl acetate), this peak must be due to some other additives or contaminants rather than trapped solvent. In a testament to the R-SoXR measurements, that peak is also observed in the reflectivity data. The good agreement of the experimental results and the calculation at large numbers of energy points especially in the near-edge region shows the accuracy of the calculation

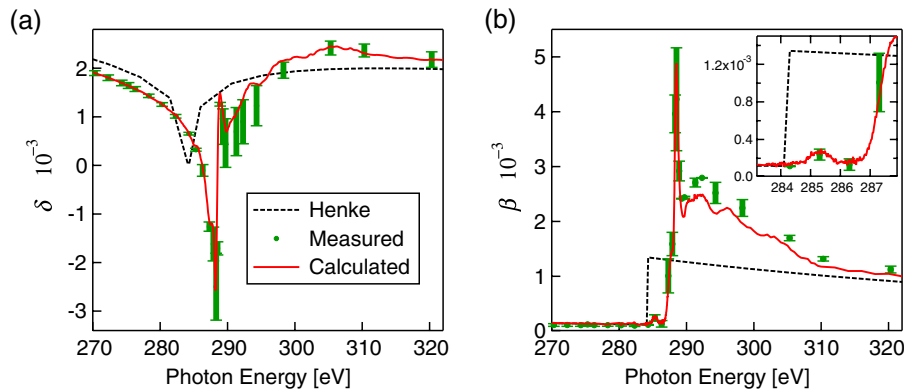


FIG. 3 (color online). Fitting results (dot) of optical constants, dispersion part δ (a), and absorption part β (b), for PMMA and calculation (solid line) using the Kramers-Kronig relations. The corresponding values derived from the Henke database are shown for comparison (dashed line). The inset in (b) zooms in on the small absorption peak at around 285 eV due to impurities or additives.

and the validity of the calculated value through the whole energy range. The optical constants of another sample polymer polystyrene were also calculated and compared to experimentally derived values with good overall correspondence, indicating that the method is generally applicable. For details see the Supplemental Material [31].

In conclusion, the indexes of refraction of a PMMA and a polystyrene thin film were measured accurately for soft x-ray energies across the carbon $1s$ absorption edge using the inherent interferometric aspects of a reflectivity measurement from a thin film. Such a measurement is simpler and more straightforward to accomplish than a number of prior methods utilized to measure δ . The values of δ calculated with the DSKK method from measured β and a few calibrated δ 's, and hence indirectly the accuracy of the NEXAFS spectrum, were verified at several energies by comparing with the experimental values of δ and β obtained from fitting the reflectance data using a least-squares fitting algorithm. The use of the DSKK method is straightforward, yet decreases the error due to the limited energy range of β . By utilizing the presented method that combines NEXAFS measurements, the Henke atomic scattering factor database, reflectivity measurements, and the Kramers-Kronig calculations, the index of refraction of polymer thin films can be determined with good accuracy in a self-consistent fashion without the need of independent mass thickness measurements. The dispersive properties of organic materials can now be tabulated in analogy to the databases already existing for β . With the necessity of access to a synchrotron facility acknowledged, the generality of this method should be applicable to a broad range of soft and hard materials.

The authors are grateful for the supplying of PMMA samples by C. R. McNeill (Monash University, Australia) and the fruitful discussions with B. Watts (PSI, Switzerland), E. M. Gullikson (ALS 6.3.2, CXRO), and A. L. D. Kilcoyne (ALS 5.3.2.2). Work at NCSU is supported by the U. S. Department of Energy under Contract

No. DE-FG02-98ER45737. Data were acquired at beam lines 5.3.2.2 and 6.3.2 at the ALS, which is supported by the Director of the Office of Science, Department of Energy, under Contract No. DE-AC02-05CH11231.

*Present address: Department of Physics, University of Illinois at Urbana-Champaign, Urbana, Illinois 61801, USA.

- [1] B. L. Henke, E. M. Gullikson, and J. C. Davis, *At. Data Nucl. Data Tables* **54**, 181 (1993).
- [2] O. Dhez, H. Ade, and S. Urquhart, *J. Electron Spectrosc. Relat. Phenom.* **128**, 85 (2003).
- [3] J. Kikuma and B. P. Tonner, *J. Electron Spectrosc. Relat. Phenom.* **82**, 53 (1996).
- [4] B. Watts, S. Swaraj, D. Nordlund, J. Lüning, and H. Ade, *J. Chem. Phys.* **134**, 024702 (2011).
- [5] S. Urquhart, A. P. Hitchcock, A. P. Smith, H. W. Ade, W. Lidy, E. G. Rightor, and G. E. Mitchell, *J. Electron Spectrosc. Relat. Phenom.* **100**, 119 (1999).
- [6] S. Urquhart and H. Ade, *J. Phys. Chem. B* **106**, 8531 (2002).
- [7] P. L. Cook, X. Liu, W. Yang, and F. J. Himpsel, *J. Chem. Phys.* **131**, 194701 (2009).
- [8] K. Kaznatcheyev, A. Osanna, C. Jacobsen, O. Plashkevych, O. Vahtras, H. Ågren, V. Carravetta, and A. P. Hitchcock, *J. Phys. Chem. A* **106**, 3153 (2002).
- [9] S. Dambach *et al.*, *Phys. Rev. Lett.* **80**, 5473 (1998).
- [10] D. Joyeux, F. Polack, and D. Phalippou, *Rev. Sci. Instrum.* **70**, 2921 (1999).
- [11] C. Jacobsen, S. Y. Wang, W. Yun, S. Frigo, R. Soufli, and J. F. Seely, *Proc. SPIE Int. Soc. Opt. Eng.* **5538**, 23 (2004).
- [12] C. Wang, T. Araki, and H. Ade, *Appl. Phys. Lett.* **87**, 214109 (2005).
- [13] S. Swaraj, C. Wang, H. Yan, B. Watts, J. Lüning, C. R. McNeill, and H. Ade, *Nano Lett.* **10**, 2863 (2010).
- [14] H. Yan, S. Swaraj, C. Wang, I. Hwang, N. C. Greenham, C. Groves, H. Ade, and C. R. McNeill, *Adv. Funct. Mater.* **20**, 4329 (2010).

- [15] M. Mezger, B. Jérôme, J.B. Kortright, M. Valvidares, E.M. Gullikson, A. Giglia, N. Mahne, and S. Nannarone, *Phys. Rev. B* **83**, 155406 (2011).
- [16] C. Wang, D.H. Lee, A. Hexemer, M.I. Kim, W. Zhao, H. Hasegawa, H. Ade, and T.P. Russell, *Nano Lett.* **11**, 3906 (2011).
- [17] B.A. Collins *et al.*, *Nat. Mater.* **11**, 536 (2012).
- [18] E. Gann, A.T. Young, B.A. Collins, H. Yan, J. Nasiatka, H.A. Padmore, H. Ade, A. Hexemer, and C. Wang, *Rev. Sci. Instrum.* **83**, 045110 (2012).
- [19] M. Beckers, T. Senkbeil, T. Gorniak, M. Reese, K. Giewekemeyer, S.-C. Gleber, T. Salditt, and A. Rosenhahn, *Phys. Rev. Lett.* **107**, 208101 (2011).
- [20] J. Stöhr, *NEXAFS Spectroscopy* (Springer, New York, 1992).
- [21] H. Ade, A.P. Smith, H. Zhang, G.R. Zhuang, J. Kirz, E. Rightor, and A. Hitchcock, *J. Electron Spectrosc. Relat. Phenom.* **84**, 53 (1997).
- [22] E.M. Gullikson, P. Denham, S. Mrowka, and J.H. Underwood, *Phys. Rev. B* **49**, 16283 (1994).
- [23] B. Sae-Lao and R. Soufli, *Appl. Opt.* **41**, 7309 (2002).
- [24] R. Soufli and E.M. Gullikson, *Appl. Opt.* **37**, 1713 (1998).
- [25] K. Rosfjord, C. Chang, R. Miyakawa, H. Barth, and D. Attwood, *Appl. Opt.* **45**, 1730 (2006).
- [26] H.-J. Hagemann, W. Gudat, and C. Kunz, *J. Opt. Soc. Am.* **65**, 742 (1975).
- [27] J. Svatos, D. Joyeux, D. Phalippou, and F. Polack, *Opt. Lett.* **18**, 1367 (1993).
- [28] R. Soufli and E.M. Gullikson, *Appl. Opt.* **36**, 5499 (1997).
- [29] C. Chang, E. Anderson, P. Naulleau, E. Gullikson, K. Goldberg, and D. Attwood, *Opt. Lett.* **27**, 1028 (2002).
- [30] R. de L. Kronig, *J. Opt. Soc. Am.* **12**, 547 (1926).
- [31] See Supplemental Material <http://link.aps.org/supplemental/10.1103/PhysRevLett.110.177401> for detailed mathematical equations and procedures, experimental details, and the optical constants measurements of polystyrene.
- [32] R. Bachrach and F. Brown, *Phys. Rev. B* **1**, 818 (1970).
- [33] K.F. Palmer, M.Z. Williams, and B.A. Budde, *Appl. Opt.* **37**, 2660 (1998).
- [34] A.L.D. Kilcoyne *et al.*, *J. Synchrotron Radiat.* **10**, 125 (2003).
- [35] J.H. Underwood and E.M. Gullikson, *J. Electron Spectrosc. Relat. Phenom.* **92**, 265 (1998).
- [36] T. Coffey, S. Urquhart, and H. Ade, *J. Electron Spectrosc. Relat. Phenom.* **122**, 65 (2002).
- [37] D.L. Windt, *Comput. Phys.* **12**, 360 (1998).
- [38] J. Perlich, V. Körstgens, E. Metwalli, L. Schulz, R. Georgii, and P. Müller-Buschbaum, *Macromolecules* **42**, 337 (2009).
- [39] X. Zhang, K.G. Yager, S. Kang, N.J. Fredin, B. Akgun, S. Satija, J.F. Douglas, A. Karim, and R.L. Jones, *Macromolecules* **43**, 1117 (2010).